DRAFT VERSION JANUARY 15, 2025
Typeset using LaTeX **twocolumn** style in AASTeX63

A Spin on StrayCats: Utilizing *NuSTAR* intentional stray light observations to measure the spin of MAXI J1535-571

CALLIE COLLINS,[1] R. M. LUDLAM,[1] S. LI,[1] & COLLABORATORS,

[1]*Department of Physics & Astronomy, Wayne State University, 666 West Hancock Street, Detroit, MI 48201, USA*

1. INTRODUCTION

Astrophysical black holes can be fully described when both their mass (M_{BH}) and dimensionless spin parameter (a) are known. The latter is the mass normalized description of the total angular momentum of the compact object ($a = cJ/GM_{BH}^2$, where c is the speed of light, G is the gravitational constant, and J is the angular momentum). MAXI J1535-571 is a transiently accreting black hole discovered by Monitor of All-sky X-ray Image (*MAXI*) on September 2, 2017 (Negoro et al. 2017). It had an active accretion episode where material was transferred from a stellar companion to the compact object through an accretion disk. The source has previously been studied using data from other missions such as the Neutron star Interior Composition ExploreR (*NICER*; Gendreau et al. 2012), for which the dimensionless spin parameter has been estimated to be consistent with a near-maximally spinning black hole (Miller et al. 2018) through the use of 'relativistic reflection' models. These models fit the relativistic effects imparted onto emission lines observed in X-ray spectra. The iron (Fe) K emission lines emitted between 6.4–6.97 keV are intrinsically narrow but broadened due to strong gravity affecting the innermost regions of the accretion disk close to the black hole (Fabian et al. 2000). The degree of broadening in the emission lines correlates with proximity, and gives a direct indication of the inner disk radius, which directly relates to the dimensionless spin parameter (a) since higher values of spin can support orbit in the disk closer to the compact object (Reynolds 2021).

The Nuclear Spectroscopic Telescope Array, nicknamed *NuSTAR* (Harrison et al. 2013), has two focal plane modules (FPMA and FPMB) onboard and is the first hard X-ray focusing satellite in orbit, which can focus photons from 3–79 keV. It's primary objective since it's launch in 2012 was to "study... hard X-ray emitting compact objects in the Galaxy by mapping central regions of the Milky Way" (Harrison et al. 2013). However, because the mast between the focusing optics and the detectors isn't enclosed, X-rays from nearby bright objects are able to pass through the gap between the optics and the aperture stop and directly illuminate the detectors at off-axis angles of 1–4° in a given observation of a densely crowded area (Madsen et al. 2017). The sources of stray light have been identified and cataloged in what is called the *NuSTAR* Straylight Catalog, or StrayCats (Grefenstette et al. 2021), which as of July of 2022 had 862 entries (Ludlam et al. 2022). Ten of those entries are attributed to MAXI J1535-571, however, only eight of which have an illuminated area on the detectors larger than > 1 cm^2 that are useful for extracting higher level science products. These observations are classified as intentional stray light since they were scheduled by the mission to reduce the data telemetry load to avoid onboard data loss between the passage of downlink stations.

As mentioned previously, the spin of MAXI J1535-571 is consistent with a near-maximally spinning black hole with $a \geq 0.84$ (Miller et al. 2018; Xu et al. 2018; Dong et al. 2022; Ma et al. 2024) via *NICER* and focused *NuSTAR* data. Calculating the dimensionless spin parameter of MAXI J1535-571 using StrayCats data presents a novel approach of gathering information about black holes from X-ray emissions. Additionally, since the photons do not pass through the focusing optics, data can be collected from the source up to 120 keV (Mastroserio et al. 2022). Not only does this broaden the scope of the types of objects that can be studied by *NuSTAR* than what was initially intended, it also poses a more efficient method of data collection.

2. OBSERVATIONS AND DATA REDUCTION

MAXI J1535-571 was observed with *NuSTAR* as intentional stray light with an illumination pattern > 1 cm^2 on four occasions during the 2017 outburst. Figure 1 indicates where these observations occurred with respect to the long-term *MAXI* light curve. Table 1 provides further information about each observation. The data were reduced using NUSTARDAS v.2.1.2 and stray light wrappers available in nustar-gen-utils[1]. We utilize the source region files provided by StrayCats II[2] (Ludlam et al. 2022) to extract light curves and spectra for each observation. The spectra are optimally binned (Kaastra & Bleeker 2016) via FTGROUPPHA. The light curves, hardness ratio (8–13 keV/3–8 keV), and hardness-intensity diagram are shown in Figure 2 for each observation. We note that light curves and spectra cannot be extracted for the stray light data by using an extraction region in a 'source-free' area of the detectors (Grefenstette et al. 2021; Mastroserio et al. 2022). Similar to previous literature performing spectral analysis of stray light data (Mastroserio et al. 2022; Yun et al. 2023), the background is modeled using NUSKYBGD[3] (Wik et al. 2014), which is a piece-wise model of the various background components for *NuSTAR*. Given that the observations do not pass through the focusing

[1] https://github.com/NuSTAR/nustar-gen-utils/

[2] https://nustarstraycats.github.io/straycats/

[3] https://github.com/NuSTAR/nuskybgd-py

Table 1. Observation information for *NuSTAR* intentional stray light of MAXI J1535-571

Obs#	ObsID	Obs Date	FPM	StrayID	Area	Exp. (ks)
1	80302310002	2017-09-17	A	StrayCatsI_201	3.3	6.18
			B	StrayCatsI_202	7.4	5.90
2	80302310004	2017-09-21	A	StrayCatsI_199	2.2	6.14
			B	StrayCatsI_200	7.2	5.60
3	80302312001	2017-10-23	A	StrayCatsI_205	6.8	9.53
			B	StrayCatsI_206	6.8	9.49
4	80302312002	2017-10-25	A	StrayCatsI_203	6.9	12.89
			B	StrayCatsI_204	6.9	12.75

Note.— The StrayID refers to the row number in `StrayCats`. The illuminating area of each stray light pattern is given in units of cm^2.

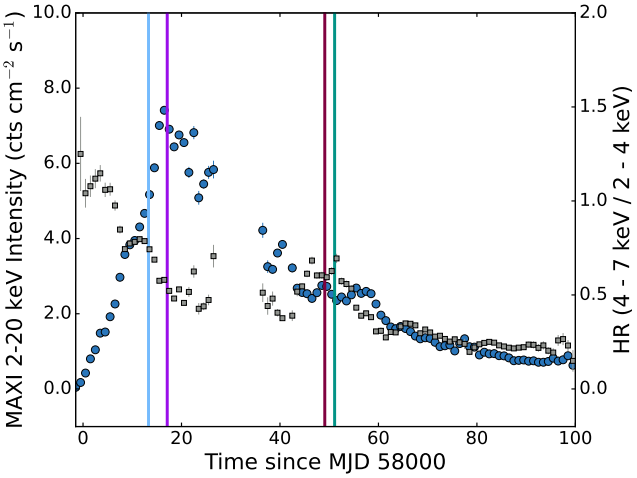

Figure 1. *MAXI* light curve (blue circles) of the 2017 outburst of MAXI J1535-571. The grey squares points indicate the hardness ratio (HR) of the source throughout the outburst as calculated using the 4–7 keV and 2–4 keV bands of *MAXI*. The vertical solid lines indicate the dates of the *NuSTAR* intentional stray light observations of interest.

optics nor occur during enhanced solar activity, we do not include the focused cosmic X-ray background (CXB) or solar background component in our background treatment.

3. ANALYSIS AND RESULTS

Spectral analysis was performed via XSPEC using cash statistics. All spectra were modeled in the 3–160 keV energy band (though we note that 120–160 keV contains only instrumental noise and is used to fit the internal continuum component of the background). An absorbed (TBABS) power law with an exponential cutoff energy (CUTOFFPL) was first applied to all four observations individually, with the equivalent hydrogen column was frozen at a value of 1.4 from galactic HI surveys (HI4PI Collaboration et al. 2016). The CUTOFFPL model alone was poorly fit on the second observation. From Figure 1 and Figure 2, this observation occurred at the peak of the outburst and has a lower HR than the other observations, thus occupies a softer spectral state that would have enhanced thermal emission from the accretion disk. For this observation, a multi-color blackbody (DISKBB) component was added to account for the thermal emission from the accretion disk. The final spectral models

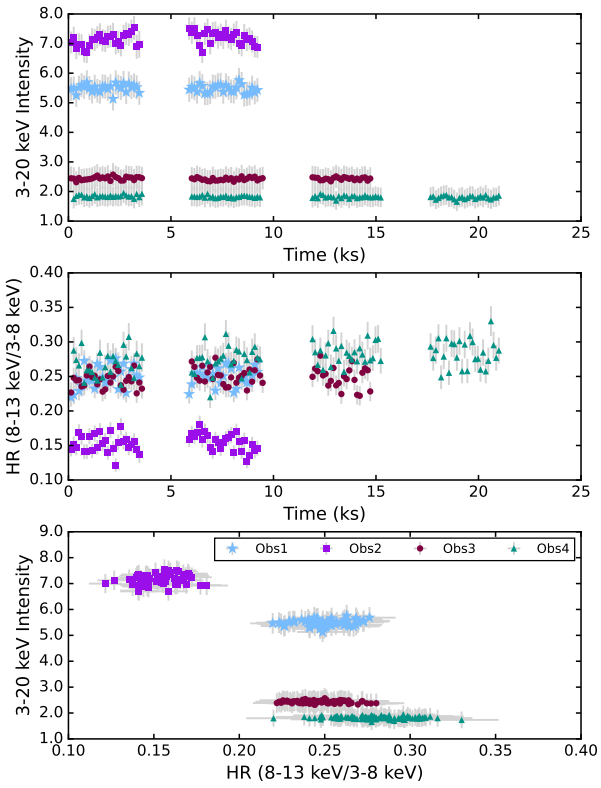

Figure 2. The light curves and hardness ratio (HR) for each intentional stray light observation of MAXI J1535-571. The intensity is normalized to the area of the stray light pattern, thus the units are counts s^{-1} cm^{-2}. Data are binned at 128 s and only one FPM is shown for clarity.

Table 2. Continuum modeling of each observation

Model	Parameter	Obs1	Obs2	Obs3	Obs4
TBABS	$N_{\rm H}^{\dagger}$ (10^{22} cm^{-2})		1.4		
DISKBB	kT (keV)	–	1.31 ± 0.01	–	–
	norm	–	1666 ± 124	–	–
CUTOFFPL	Γ	2.24 ± 0.01	$2.31^{+0.06}_{-0.07}$	2.36 ± 0.01	2.18 ± 0.01
	$E_{\rm cut}$ (keV)	35 ± 1	37^{+5}_{-4}	92^{+9}_{-8}	69^{+5}_{-4}
	norm	56 ± 1	45 ± 6	26.9 ± 0.4	18.7 ± 0.3
	c-stat/d.o.f	962.8/615	659.5/592	976.3/647	1023/659

† = fixed

Note.— Errors are reported at the 90% confidence level.

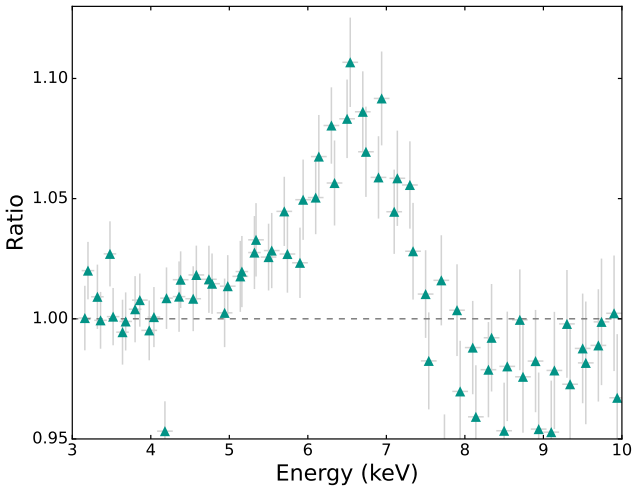

Figure 3. Example of the broad Fe line residual present in the FPMA and FPMB stray light data by taking the ratio of stray light data from Obs 4 to the simple continuum model.

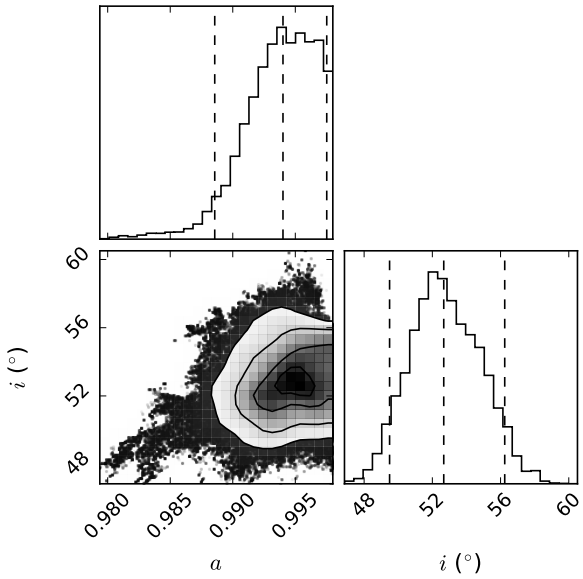

Figure 4. Best fit constraints on spin, a, and inclination, i, of MAXI J1535-571 derived via MCMC for the joint spectral modeling of all observations. The 2D contours represent the 1σ, 1.5σ, and 2σ confidence levels. The dashed vertical lines in the 1D distributions for each parameter correspond to the 0.05, 0.50, and 0.95 quantiles.

for Obs1, Obs3, and Obs4 were TBABS*(CUTOFFPL), and for Obs2 TBABS*(DISKBB+CUTOFFPL). The results of the continuum fitting can be seen in Table 2.

All four observations contained a broad, assymetric Fe line profile in the stray light data (see Figure 3 for an example), hence we apply the self-consistent relativistic reflection model RELXILL (García et al. 2013, 2014) to the spectra. This model includes both the illuminating cutoff power law component in addition to the reflection, so we remove the CUTOFFPL component from the continuum model when RELXILL is used. The model consists of the following parameters: inner emissivity index (q_1), outer emissivity index (q_2), break radius where the emissivity index changes ($R_{\rm break}$) in units of gravitational radii ($R_g = GM/c^2$), dimensionless spin (a), inclination (i) in degrees, inner disk radius ($R_{\rm in}$) in units of innermost stable circular orbit ($R_{\rm ISCO}$), outer disk radius ($R_{\rm out}$) in R_g, the redshift (z) to the source, the photon index of the illuminating power law distribution of photons from the corona (Γ), the ionization state of the material ($\log(\xi)$), the abundance of Fe in the disk relative to solar values (A_{Fe}), cut off energy of the power law ($E_{\rm cut}$), and reflection fraction to quantify the amount of photons from the illuminating corona that interact with the disk versus escape to infinity ($f_{\rm refl}$). We fix the break radius at 10, redshift to 0 since the source is in our galaxy and not subject to cosmological redshift, inner disk radius at 1 $R_{\rm ISCO}$, outer disk radius at 1000 R_g. The final spectral model was TBABS*(RELXILL) with a DISKBB component applied in Obs2.

The data were modeled simultaneously for all epochs with key parameters (a, i, A_{Fe}) tied since they should not change between observations. Considering the large number of parameters, a Markov Chain Monte Carlo (MCMC) was run with 100 walkers for a chain length of 10^6 and a burn-in

Table 3. Simultaneous reflection modeling of all four intentional stray light observations

Model	Parameter	Obs1	Obs2	Obs3	Obs4
TBABS	$N_{\rm H}^{\dagger}$ (10^{22} cm^{-2})		1.4		
DISKBB	kT (keV)	–	$1.479^{+0.05}_{-0.04}$	–	–
	norm	–	766^{+143}_{-151}	–	–
RELXILL	q_1	$6.46^{+0.76}_{-0.02}$	9.5 ± 0.3	$7.7^{+0.3}_{-0.6}$	$6.16^{+0.70}_{-0.01}$
	q_2	$0.832^{+0.1}_{-0.3}$	$0.29^{+0.06}_{-0.04}$	$0.6^{+0.3}_{-0.1}$	$1.2^{+0.1}_{-0.3}$
	$R_{\rm break}^{\dagger}$		10		
	a		$0.996^{+0.001}_{-0.008}$		
	i (°)		51^{+4}_{-3}		
	Γ	$2.05^{+0.02}_{-0.04}$	$2.41^{+0.07}_{-0.04}$	$2.25^{+0.04}_{-0.03}$	$2.21^{+0.03}_{-0.05}$
	$\log(\xi)$	$4.6^{+0.1}_{-0.2}$	$4.0^{+0.4}_{-0.2}$	$3.9^{+0.3}_{-0.2}$	$3.2^{+0.2}_{-0.1}$
	A_{Fe}		2.58 ± 0.6		
	$E_{\rm cut}$ (keV)	40^{+2}_{-3}	75^{+22}_{-5}	84^{+14}_{-8}	77 ± 7
	$f_{\rm refl}$	$2.5^{+0.4}_{-0.2}$	$4.6^{+0.8}_{-03}$	$1.2^{+0.1}_{-0.3}$	0.7 ± 0.1
	norm	0.14 ± 0.01	$0.28^{+0.03}_{-0.07}$	$0.16^{+0.03}_{-0.02}$	$0.18^{+0.01}_{-0.02}$
	$F_{3-120\ \rm keV}$	1.00 ± 0.07	$1.1^{+0.2}_{-0.4}$	$0.48^{+0.09}_{-0.06}$	$0.48^{+0.03}_{-0.05}$
	c-stat/d.o.f		2785/2495		

† = fixed

Note.— The inner disk radius $R_{\rm in}$ is fixed a 1 $R_{\rm ISCO}$. The outer disk radius is fixed at 1000 R_g. The redshift z is fixed at 0 since the source is galactic. $F_{3-120\ \rm keV}$ indicates the unabsorbed flux from 3–120 keV in units of 10^{-7} erg s^{-1} cm^{-2}.

of 10^6 in order to explore the parameter space and find the global best fit to the data. Figure 4 shows the resulting best fit values for the inclination and dimensionless spin parameter. The stray light data again confirm that MAXI J1535-571 is a near-maximally spinning black hole with the spin parameter measured at a value of $a = 0.996^{+0.002}_{-0.006}$. The model also yielded an inclination of $\sim 51°$, which is within the range of previous measurements (Miller et al. 2018; Xu et al. 2018).

4. DISCUSSION

We performed the first spectral analysis of four intentional stray light observations of MAXI J1535-571 taken with *NuSTAR* during its 2017 outburst. A strong Fe line is present in the spectra. Through the application of reflection models to account for general relativistic effects imparted on the emission line, we were able to constrain key parameters like the inclination of the system and the dimensionless spin parameter. Intentional stray light observations of MAXI J1535-571 were able to confirm that it is a near-maximally spinning black hole in agreement with literature (Miller et al. 2018; Xu et al. 2018; Dong et al. 2022; Ma et al. 2024). The measured inclination of the object was also consistent with previous literature that reports a moderate inclination (Miller et al. 2018; Xu et al. 2018). Thus, it can be concluded that stray light is a viable source of data for performing spin estimates for bright black hole X-ray binaries in outburst, which would reduce the telemetry load aboard *NuSTAR* and allow for longer observations. Moreover, the data was viable above the nominal 79 keV limit for focused *NuSTAR* data, thus could have important implications for constraining high energy emission in black hole systems. As of July of 2022, the 862 stray light observations made by *NuSTAR* have been attributed to 83 objects (Ludlam et al. 2022). As the telescope continues to orbit and take observations, that number will continue to grow. Other intentional stray light observations could be valuable for future scientific research.

REFERENCES

Dong, Y., Liu, Z., Tuo, Y., et al. 2022, MNRAS, 514, 1422, doi: 10.1093/mnras/stac1466

Fabian, A. C., Iwasawa, K., Reynolds, C. S., & Young, A. J. 2000, PASP, 112, 1145, doi: 10.1086/316610

García, J., Dauser, T., Reynolds, C. S., et al. 2013, ApJ, 768, 146, doi: 10.1088/0004-637X/768/2/146

García, J., Dauser, T., Lohfink, A., et al. 2014, ApJ, 782, 76, doi: 10.1088/0004-637X/782/2/76

Gendreau, K. C., Arzoumanian, Z., & Okajima, T. 2012, in Society of Photo-Optical Instrumentation Engineers (SPIE) Conference Series, Vol. 8443, Space Telescopes and Instrumentation 2012: Ultraviolet to Gamma Ray, ed. T. Takahashi, S. S. Murray, & J.-W. A. den Herder, 844313, doi: 10.1117/12.926396

Grefenstette, B. W., Ludlam, R. M., Thompson, E. T., et al. 2021, ApJ, 909, 30, doi: 10.3847/1538-4357/abe045

Harrison, F. A., Craig, W. W., Christensen, F. E., et al. 2013, ApJ, 770, 103, doi: 10.1088/0004-637X/770/2/103

HI4PI Collaboration, Ben Bekhti, N., Flöer, L., et al. 2016, A&A, 594, A116, doi: 10.1051/0004-6361/201629178

Kaastra, J. S., & Bleeker, J. A. M. 2016, A&A, 587, A151, doi: 10.1051/0004-6361/201527395

Ludlam, R. M., Grefenstette, B. W., Brumback, M. C., et al. 2022, ApJ, 934, 59, doi: 10.3847/1538-4357/ac7b27

Ma, R., Tao, L., Méndez, M., et al. 2024, MNRAS, 528, 3864, doi: 10.1093/mnras/stae291

Madsen, K. K., Christensen, F. E., Craig, W. W., et al. 2017, Journal of Astronomical Telescopes, Instruments, and Systems, 3, 044003, doi: 10.1117/1.JATIS.3.4.044003

Mastroserio, G., Grefenstette, B. W., Thalhammer, P., et al. 2022, ApJ, 941, 35, doi: 10.3847/1538-4357/ac8c94

Miller, J. M., Gendreau, K., Ludlam, R. M., et al. 2018, ApJL, 860, L28, doi: 10.3847/2041-8213/aacc61

Negoro, H., Ishikawa, M., Ueno, S., et al. 2017, The Astronomer's Telegram, 10699, 1

Reynolds, C. S. 2021, ARA&A, 59, 117, doi: 10.1146/annurev-astro-112420-035022

Wik, D. R., Hornstrup, A., Molendi, S., et al. 2014, ApJ, 792, 48, doi: 10.1088/0004-637X/792/1/48

Xu, Y., Harrison, F. A., García, J. A., et al. 2018, ApJL, 852, L34, doi: 10.3847/2041-8213/aaa4b2

Yun, S. B., Grefenstette, B. W., Ludlam, R. M., et al. 2023, ApJ, 947, 81, doi: 10.3847/1538-4357/acb689